Supporting Information

High interfacial storage capability of porous NiMn2O4/C hierarchical tremella-like nanostructures as lithium ion battery anode

Wenpei Kang[a], Yongbing Tang[a,b]*, Wenyue Li[a,b], Xia Yang[a], Hongtao Xue[a], Qingdan Yang[a], and Chun-Sing Lee[a]*

a Department of Physics and Materials Science and Center of Super-Diamond and Advanced Films (COSDAF), City University of Hong Kong, Hong Kong SAR, People's Republic of China.

b Functional Thin Films Research Center, Shenzhen Institutes of Advanced Technology, Chinese Academy of Sciences, People's Republic of China.

*Corresponding author.

E-mail: tangyb@siat.ac.cn; apcslee@cityu.edu.hk; Tel: +852-34427826

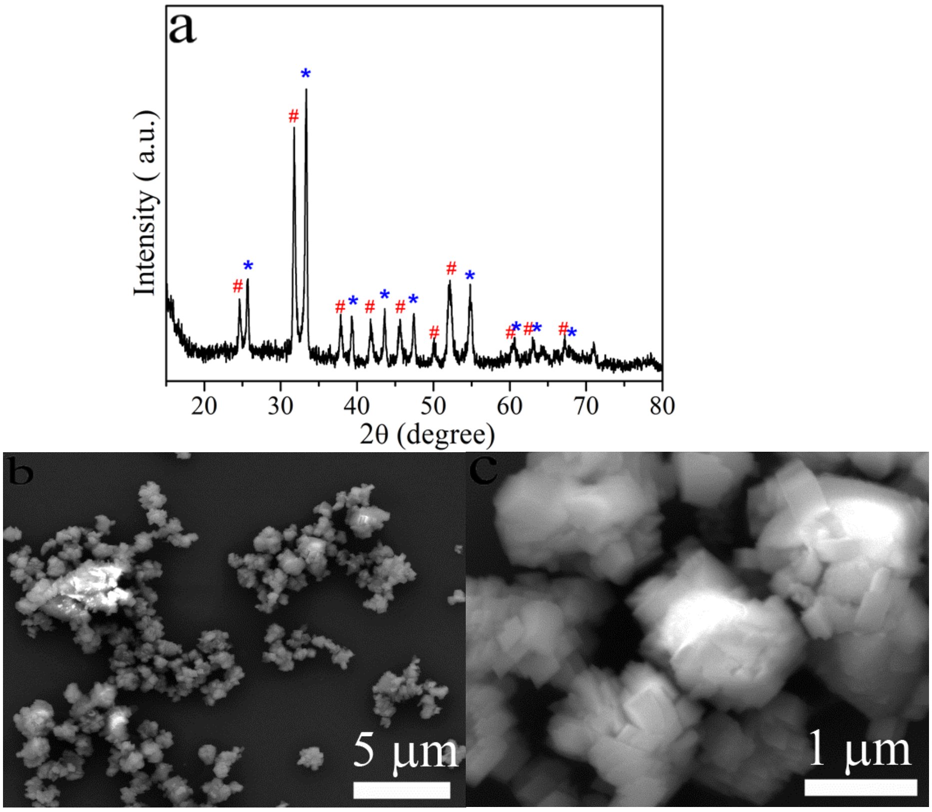

Fig. S1 (a) XRD and (b) SEM images of the carbonate precursor formed in the water. The divided XRD patterns indicate that the obtained carbonate precipitate is a mixture of $NiCO_3$ (# JCPDS No: 78-0210) and $MnCO_3$ (* JCPDS No: 86-0173), indicating the importance of TEG for the preparation of bimetallic carbonate precursor. And the morphology of the carbonate precipitate is irregular aggregate.

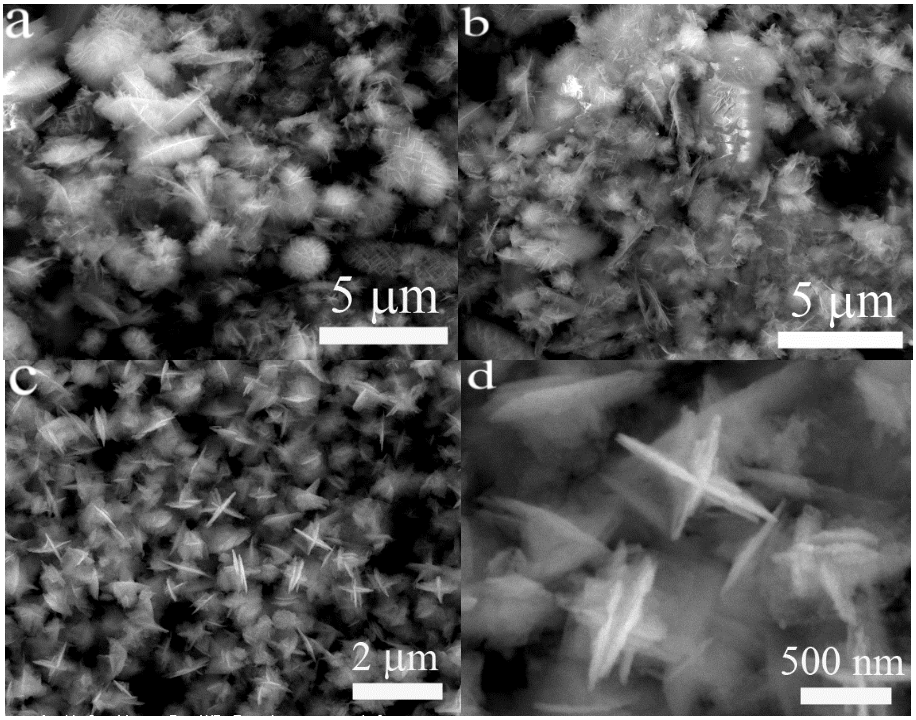

Fig. S2 SEM images of the carbonate precursor obtained (a, b) in TEG and (c, d) in a solvent of TEG and water with a ratio of 1:1.

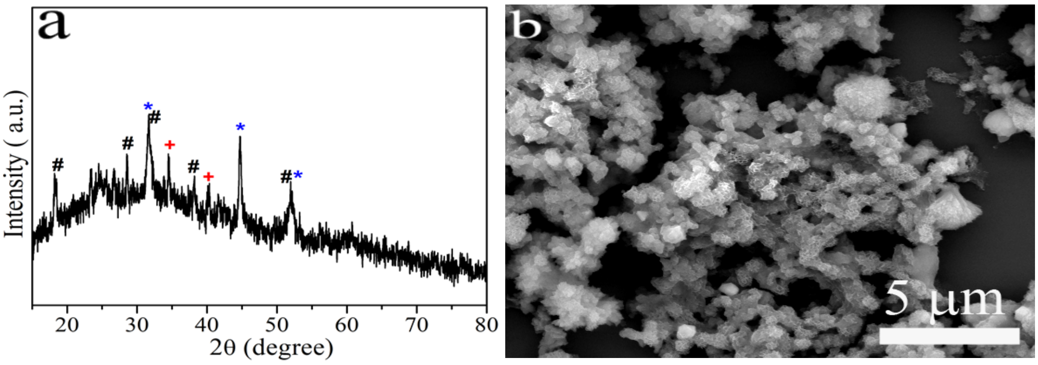

Fig. S3 (a) XRD pattern and (b) SEM images of the sample using $MnSO_4$ and $NiCl_2$ as raw materials. The obtained precipitate is a mixture of Ni_2O_3 (* JCPDS No: 14-0481), Mn_5O_8 (# JCPDS No: 39-1218) and MnO (+ JCPDS No: 07-0230).

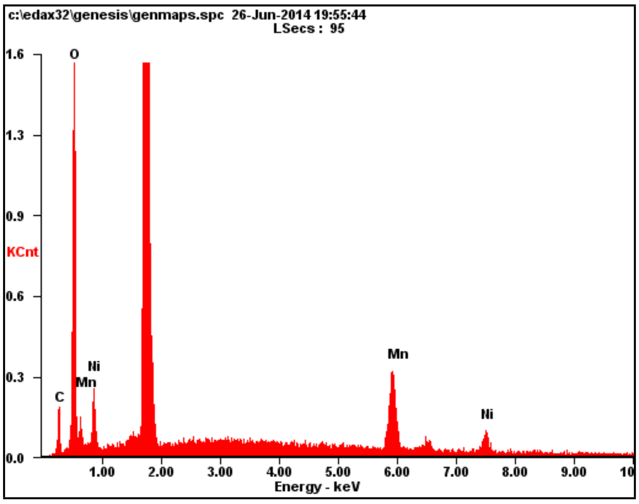

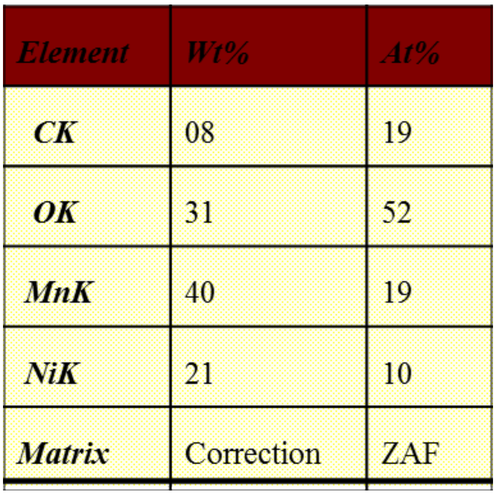

Element	Wt%	At%
CK	08	19
OK	31	52
MnK	40	19
NiK	21	10
Matrix	Correction	ZAF

Fig. S4 Energy dispersive spectroscopy (EDS) of the carbonate precursor, the elements of C, O, Mn and Ni can be detected and the strong peak is attributed to the Si wafer. The ratio of Mn and Ni is about 2:1, based on which the precursor can be confirmed as $Ni_{1/3}Mn_{2/3}CO_3$.

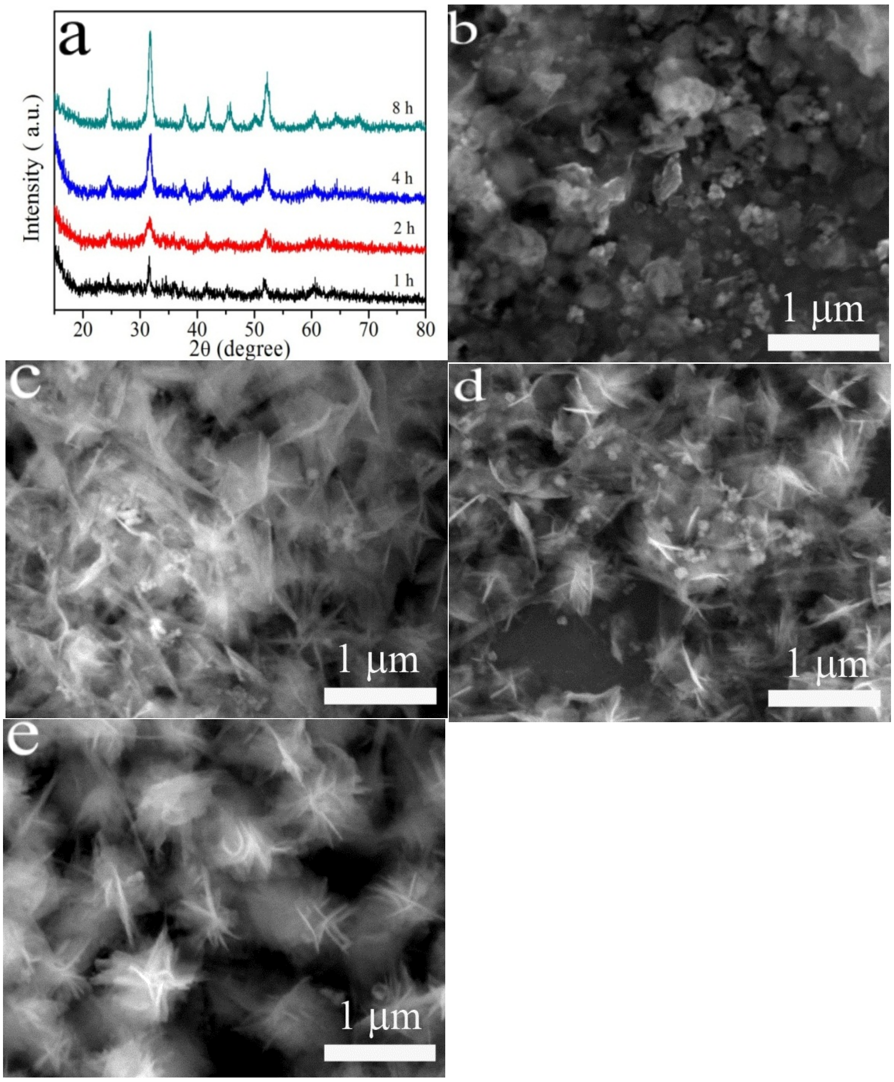

Fig. S5 (a) XRD patterns of the XRD pattern of the samples obtained after different reaction durations; SEM images of the samples prepared at 180 ºC for 1 h (a), 2 h (b); 4.0 h (c), 8 h (d).

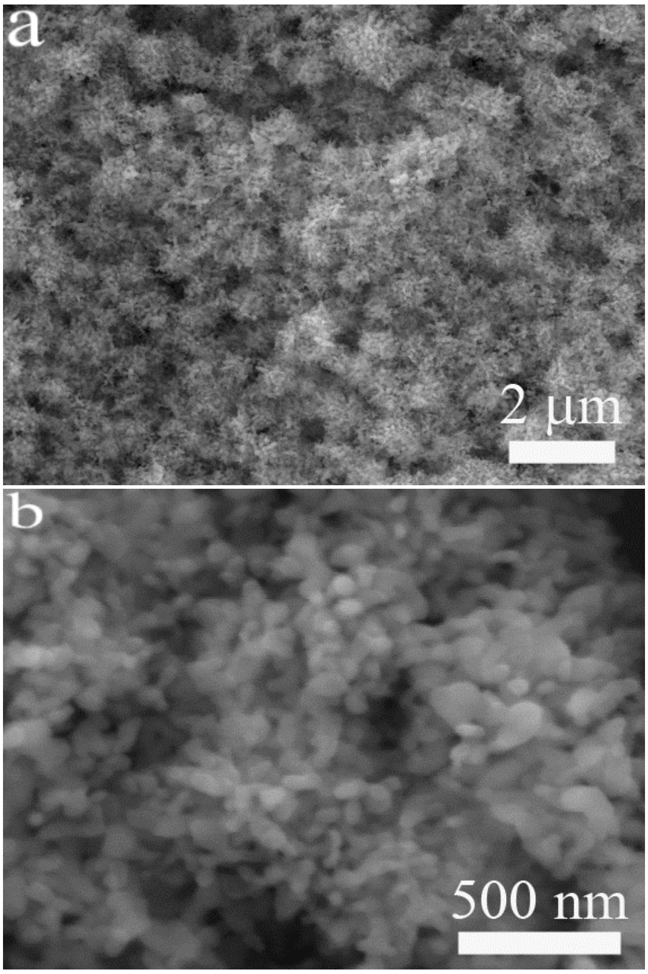

Fig. S6 SEM images of the sample obtained from heat treatment of $Ni_{1/3}Mn_{2/3}CO_3$ precursor without using PAN. It is clearly to see that the tremella-like structure has collapsed.

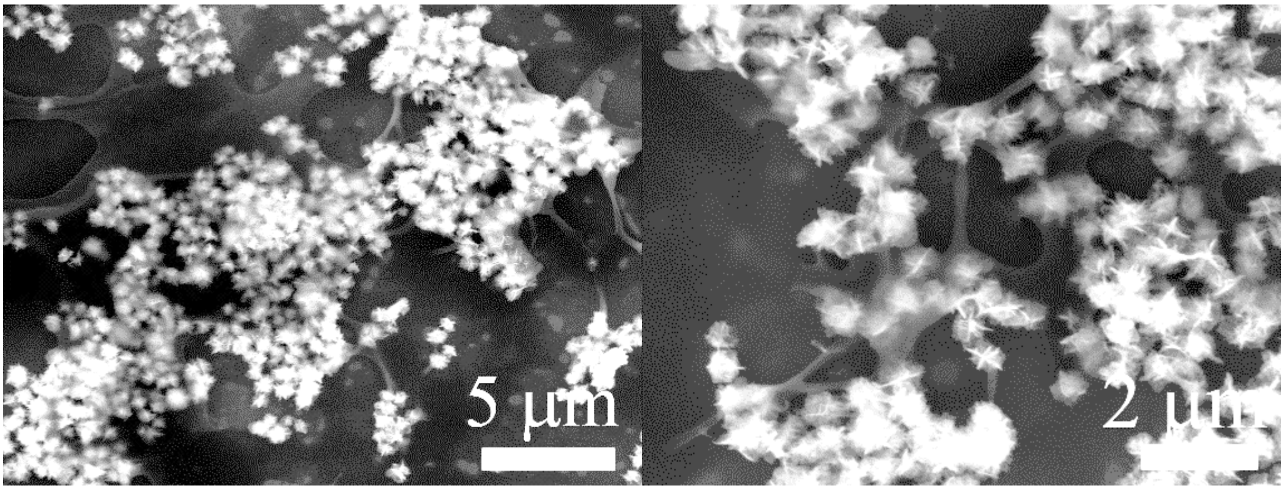

Fig. S7 SEM images after adjusting the contrast of Fig. 4a and 4b to show the carbon films more clearly.

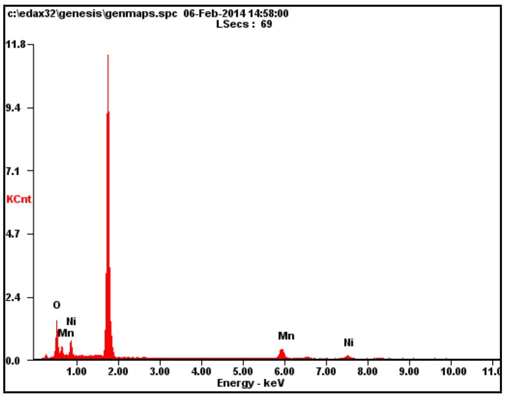

Element	***Wt%***	***At%***
OK	24	53
MnK	49	31
NiK	27	16
Matrix	Correction	ZAF

Fig. S8 Energy dispersive spectroscopy (EDS) of the $NiMn_2O_4$/C hierarchical tremella-like structures, we can obtain that the elements of C, O, Mn and Ni can be detected and the strong peak is attributed to the Si wafer. The ratio of Mn and Ni is about 2:1 which is agreement with that in the $NiMn_2O_4$.

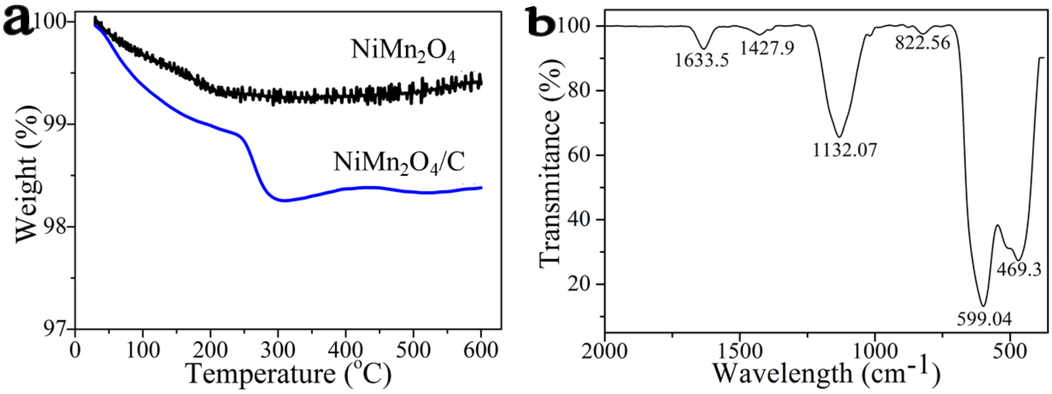

Fig. S9 Thermogravimetric analysis (TGA) results of the $NiMn_2O_4/C$ hierarchical tremella-like structures and the samples obtained obtained from heat treatment of $Ni_{1/3}Mn_{2/3}CO_3$ precursor without using PAN as shown in Fig. S6. With a quick heating step of 10 °C min^{-1} up to 600 °C, TGA analysis reveals that the carbonate-based composites can be chemically decompose between 250 and 300 °C attributed to the decomposition of the amorophous carbon. Therefore, a heat-treatment temperature of 600°C was selected for subsequent preparation of final product $NiMn_2O_4/C$. Based on the weight loss between 250-300 °C the weight fraction of C can be estimated to be 0.75%. And the curve for $NiMn_2O_4$ shows that there is no weight loss except the removal the adsorption water below 200 °C. The surface functional groups of $NiMn_2O_4/C$ composite were further analyzed by Fourier transform infrared (FT IR) spectroscopy, as shown in Fig. S9b. The observed strong band at 1132.07 cm^{-1} is attributed to the C–N stretching vibrations. The small band at 1427.9 cm^{-1} is assigned to the C=C backbone stretching vibrations. Finally, the stretching vibration of N–H groups and C–H clearly appeared at 1633.5 cm^{-1} and 822.56 cm^{-1}, respectively.[1]

a b

c d

Fig. S10 (a) SEM images of porous $NiMn_2O_4$/C tremella-like nanostructures and the corresponding elemental mappings of (b) O, (c) Ni, and (d) Mn elements.

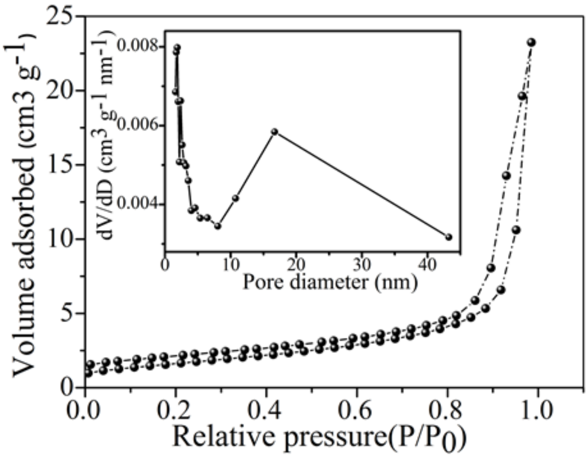

Fig. S11 N_2 adsorption–desorption isotherms with an inserted pore size distribution of porous tremella-like $NiMn_2O_4/C$ hierarchical nanostructure.

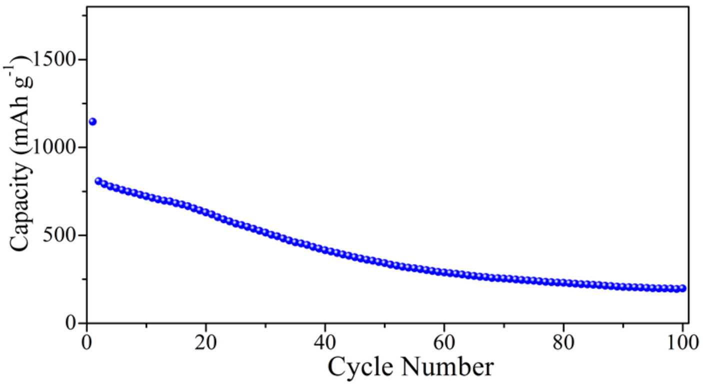

Fig S12. Cycling performance of pristine $NiMn_2O_4$ nanoparticles at a current density of 1000 mA g^{-1}. The pristine $NiMn_2O_4$ electrode shows continuously decreasing capacities. The capacity decreases to ~200 mAh g^{-1} after 100 cycles.

References:

1 A. Alabadi, X, J. Yang, Z. H. Dong, Z. Li and B. E Tan, *J. Mater. Chem. A*, 2014, **2**, 11697